

Afterglow light curves from magnetized GRB flows

Petar Mimica¹, Dimitrios Giannios² and Miguel Ángel Aloy¹

¹Departamento de Astronomía y Astrofísica, Universidad de Valencia, 46100, Burjassot, Spain
email: Petar.Mimica@uv.es

²Department of Astrophysical Sciences, Peyton Hall, Princeton University, Princeton, USA

Abstract. Using the RMHD code *MARGENESIS* and the radiative transfer code *SPEV* we compute multiwavelength afterglow light curves of magnetized ejecta of gamma-ray bursts interacting with a uniform circumburst medium. We are interested in the emission from the reverse shock when ejecta magnetization varies from $\sigma_0 = 0$ to $\sigma_0 = 1$. For typical parameters of the ejecta, the emission from the reverse shock peaks for magnetization $\sigma_0 \sim 0.01 - 0.1$, and is suppressed for higher σ_0 . We fit the early afterglow light curves of GRB 990123 and 090102 and discuss the possible magnetization of the outflows of these bursts. Finally we discuss the amount energy left in the magnetic field which is available for dissipation at later afterglow stages.

Keywords. hydrodynamics (magnetohydrodynamics:) MHD, radiation mechanisms: nonthermal, radiative transfer, shock waves, methods: numerical, gamma rays: bursts

1. Introduction

Two alternatives for creating gamma ray burst (GRB) outflows are usually considered today: a thermal energy dominated fireball (Paczynski 1986, Goodman 1986) or a Poynting-flux dominated flow (PDF; Usov 1992, Thompson 1994, Meszaros & Rees 1997). The flow magnetization parameter $\sigma_0 \ll 1$ in the fireball, and the radiation pressure accelerates the flow up to bulk Lorentz factors $\Gamma_0 \simeq h_{in}$, latter being the flow initial specific enthalpy (see e.g., Aloy, Janka & Müller 2005). PDF, on the other hand, results from a jet launched with $\sigma_{in} \gg 1$. During the process of magnetized flow acceleration a GRB emission may result from the magnetic dissipation (Thompson 1994, Spruit, Daigne & Drenkhahn 2001, Giannios 2008) or the internal shocks (Fan, Wei & Zhang 2004, Mimica & Aloy 2010). These processes are not expected to be ultra-efficient consumers of magnetic energy and we expect that the flow can still be considerably magnetized at the end of the acceleration phase ($\sigma_0 \simeq 1$) while its bulk Lorentz factor is expected to be $\Gamma_0 \simeq \sigma_{in}$ (Komissarov *et al.* 2009, Tchekhovskoy *et al.* 2009, Lyubarski 2010). However, there is currently no consensus on the exact value of σ_0 at the onset of the afterglow phase (there are scenarios where $\sigma_0 \gg 1$, see e.g., Lyutikov & Blandford 2003). Regardless of this, the mere fact that the flow is magnetized at the beginning of the afterglow should leave an imprint on the early optical light curve: if $\sigma_0 \ll 1$ a reverse shock (RS) is expected to form in the ejecta shell and a characteristic feature (a peak or a flattening of the slope) is expected in the light curve (Zhang *et al.* 2003); if $\sigma_0 \simeq 1$ then the RS might not form (Giannios *et al.* 2008) and the optical light curve is expected to lack the corresponding signature (Mimica *et al.* 2009a).

In this work we use numerical simulations to study the sensitivity of the afterglow emission on the value of σ_0 . In Sec. 2 we outline our model, and discuss the generic results of a parametric study. Application to two GRBs is detailed in Sec. 3.

2. Dependence of afterglow dynamics and emission on flow magnetization

It is generally thought that the afterglow emission of a GRB originates after the flow has been collimated and accelerated, and after the GRB prompt emission has finished. We idealize the GRB flow assuming it is composed of cold ejecta moving in a radial direction. If the ejecta is magnetized we assume that magnetic field is dominated by a toroidal component. The initial jet magnetization is parameterized via the expression $\sigma_0 \equiv B'^2/4\pi\rho c^2$, where B' and ρ are the comoving magnetic field strength and fluid density; c is the speed of light. We furthermore simplify the model by assuming that the ejecta geometry is a spherical shell of initial thickness Δ_0 at the initial radius r_0 , where we set $\Delta_0 \ll r_0$. Finally, we assume that the shell has a bulk Lorentz factor $\Gamma_0 \gg 1/\theta$, where θ is the opening angle of the jet. This means that, at least in the early phases we are interested in, the ejecta can be modeled as spherically symmetric, and two-dimensional effects such as lateral spreading can be ignored.

The difference in dynamics between the non-magnetized and magnetized ejecta evolution has been discussed in detail in Mimica *et al.* (2009a). Two crucial parameters are σ_0 and $\xi \equiv \sqrt{l/\Delta_0}\Gamma_0^{-4/3}$, where l is the Sedov length, defined as $l = (3E/4\pi n_{\text{ext}} m_p c^2)^{1/3}$, with n_{ext} being the number density of the external medium, m_p the proton mass and E the total initial ejecta energy. It has been shown analytically (Giannios *et al.* 2008) and confirmed numerically (Mimica *et al.* 2009a) that there exist regions in the $\xi - \sigma_0$ parameter space where the RS is very weak or does not form at all, and thus its observational signature is absent. Recently Mimica *et al.* (2010) we have performed a number of simulations of afterglow ejecta with σ_0 taking values 0, 10^{-4} , 10^{-3} , 10^{-2} , 10^{-1} and 1. We have computed evolution of both thin ($\xi = 1.1$) and thick ($\xi = 0.5$) shells, as in Mimica *et al.* (2009a).

These simulations, combined with the newly available *SPEV* code for computing non-thermal emission (Mimica *et al.* 2009b) has enabled us to study dependence of both dynamics and emission on the value of σ_0 . We refer to Mimica *et al.* (2010) for the technical details of the hydrodynamical simulations and the calculation of emission. In the following two subsections we discuss the observational signature of σ_0 and the long-term evolution of the magnetic energy.

2.1. Observational signatures of varying magnetization

We compute the emission from the forward shock (FS) and the RS (if present) resulting from the ejecta-medium interaction. We assume that the random magnetic field energy density is a fraction $\epsilon_B = 5 \times 10^{-3}$ of the thermal energy density and that electrons are accelerated at both shocks with a power-law energy distribution. Left panel of Fig. 1 illustrates the importance of the RS emission at early times in the optical bands (the peak seen at $\simeq 10$ seconds).

On the right panel of Fig. 1 we see total light curves for four different initial values of σ_0 . Although numerical simulations show that the RS is progressively weaker as σ_0 is increased, this effect is compensated by the brighter emission due to the increase in the magnetic field. The result is that the brightest RS flash appears for moderately magnetized ejecta (typical with $0.1 \lesssim \sigma_0 \lesssim 0.1$). For very magnetized ejecta ($\sigma_0 = 1$) the RS optical emission is several times weaker than in the non-magnetized case.

2.2. Magnetic energy evolution

Now we look into the issue of the residual magnetic energy after the ejecta has finished interacting with the external medium. If present and dissipated at later stage, this energy

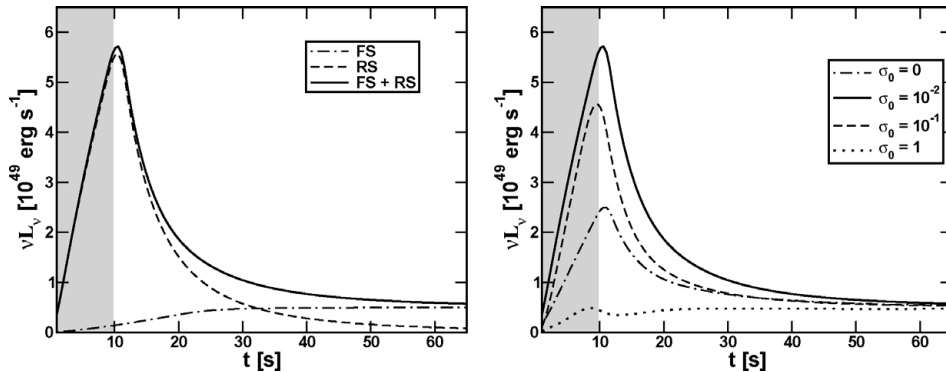


Figure 1. Left panel: R-band light curve in the GRB rest frame for the thick shell ejecta with initial magnetization $\sigma_0 = 0.01$ and Lorentz factor $\Gamma_0 = 750$. Dot-dashed and dashed lines show the FS and RS contributions, while the full line shows the total emission. The shaded region shows the observational time interval which is simultaneous with the prompt emission. Right panel: total light curves for the thick shell models $\sigma_0 = 0, 0.01, 0.1$ and 1 (dot-dashed, full, dashed and dotted lines, respectively).

may have important observational consequences for the late time emission. As is argued by Giannios (2006), ejecta deceleration might lead to the revival of current driven instabilities. Our simulations show that more than $\simeq 10$ per cent of the total ejecta energy is still in the magnetic form at the time when the RS crosses the ejecta, and is still $\simeq 2$ per cent at about 10 times the burst duration. This means that potentially there is sufficient magnetic energy at late times to be dissipated in localized reconnection regions. These might explain the afterglow X-ray flaring (Burrows *et al.* 2005) with no need for late time central engine activity.

3. Applications

In this section we focus on the optical emission from GRB 990123 (Akerlof *et al.* 1999, Briggs *et al.* 1999) and GRB 090102 (Gendre *et al.* 2009, Steele *et al.* 2009). The burst 990123 is famous because of a ninth magnitude optical flare detected few seconds after the end of the prompt emission and is one of the brightest ever detected. A recent 090102 does not show a flare, but has a $\simeq 10$ per cent polarization (an indication of large-scale magnetic fields). The duration of both bursts in the rest frame is approximately 10 seconds and, assuming the efficiency of the prompt emission of ≈ 20 per cent we estimate the isotropic equivalent ejecta energy to be 1.5×10^{55} erg for 990123 and 3×10^{54} for 090102. We use the thick shell model ($\xi < 1$) to model these bursts because the RS peak is observed close to the end of the prompt emission.

Using results of our simulations and the rescaling relations of Mimica *et al.* (2009a), we have looked for combinations of Γ_0 and σ_0 which best fit the observations. We find that for 990123 a model with $\Gamma_0 = 640$ and $\sigma_0 = 0.01$ best fits the observations, while for 090102 we get $\Gamma_0 = 940$ and $\sigma_0 = 0.1$. For both bursts we had to assume $\epsilon_B = 4 \times 10^{-7}$. The results are illustrated in Fig. 2.

The optical polarization of GRB 090102 is hard to understand as coming from the small-scale magnetic field synchrotron emission. Furthermore, it is smaller than expected from a coherent field. The polarization measured by Steele *et al.* (2009) is at a time interval $\simeq 60 - 90$ seconds in the GRB frame. As can be seen on Fig. 2, that is where the FS emission starts to dominate over the RS emission, which might indicate that 10 per

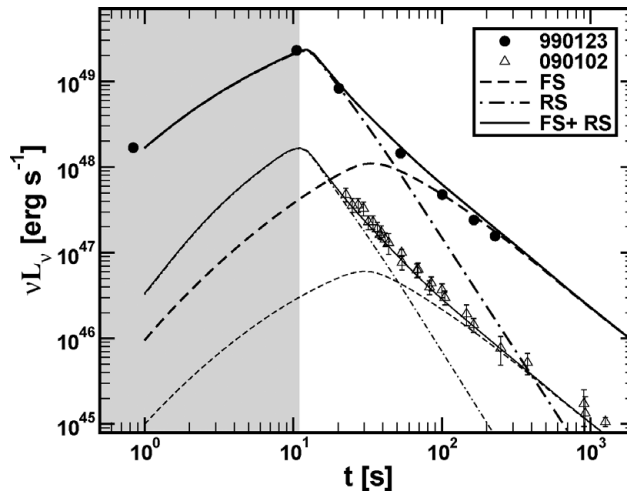


Figure 2. GRB frame R-band light curves for GRB 990123 (filled circles) and GRB 090102 (triangles), and the best fit models (lines). FS, RS and the total emission is showed by dashed, dot-dashed and full lines, respectively.

cent polarization comes from the combination of a highly polarized RS and the weakly polarized FS emission.

References

- Akerlof C., *et al.*, 1999, *Nature*, 398, 400
 Aloy M. A., Janka, H. T., Müller, E., 2005, *A&A*, 436, 273
 Briggs M. S., *et al.*, 1999, *ApJ*, 524, 82
 Burrows D. N., *et al.* 2005, *Science*, 309, 1833
 Fan Y. Z., *et al.*, 2004b, *MNRAS*, 354, 1031
 Gendre B., *et al.*, 2009, *MNRAS*, 405, 2372
 Giannios D., 2006, *A&A*, 455, L5
 Giannios D., 2008, *A&A*, 480, 305
 Giannios D., *et al.*, 2008, *A&A*, 478, 747
 Goodman J., 1986, *ApJ*, 308, L47
 Komissarov S. S., *et al.*, 2009, *MNRAS*, 394, 1182
 Lyubarsky Y. E., 2010, *MNRAS*, 402, 353
 Lyutikov M. & Blandford R., 2003, ArXiv:astro-ph/0312347
 Meszaros P. & Rees M. J., 1997, *ApJ*, 482, L29
 Mimica P. & Aloy M. A., 2010, *MNRAS*, 401, 525
 Mimica P., *et al.*, 2009a, *A&A*, 494, 879
 Mimica P., *et al.*, 2009b *ApJ*, 696, 1142
 Mimica P., *et al.*, 2010, *MNRAS*, 407, 2501
 Paczynski B., 1986, *ApJ*, 308, L43
 Spruit H. C., *et al.*, 2001, *A&A*, 369, 694
 Steele I. A., *et al.*, 2009, *Nature*, 462, 767
 Tchekhovskoy A., *et al.*, 2009, *ApJ*, 699, 1789
 Thompson C., 1994, *MNRAS*, 270, 480
 Usov V. V., 1992, *Nature*, 357, 472
 Zhang B., *et al.*, 2003, *ApJ*, 595, 950

Discussion

CASTRO-TIRADO: What are the predictions for the polarization of the reverse shock? There is already some work about this, published by D. Lazatti *et al.*

MIMICA: We did not compute the polarization of the reverse shock.